INVESTIGATION THE PUNCHING SHEAR BEHAVIOR OF REINFORCED CONCRETE SLAB-COLUMN CONNECTION USING CARBON FIBER REINFORCED POLYMERS

Dr. Ali Hameed Naser Al-Mamoori
College of Engineering, Civil Engineering Department, University of Karbala
Email address: alihameedn@@yahoo.com

ABSTRACT

The region of a slab in the vicinity of a support could fail in shear by developing a failure surface in the form a truncated cone or pyramid. This type of failure, called "Punching Shear Failure", is usually the source of collapse of flat-plate and flat-slab structures. An experiment to be conducting to investigate the punching shear strength and failure behavior of self concrete (SCC) slabs using carbon fiber reinforced polymer (CFRP) bars as internal strengthening in connection region for slab-column. Seven interior slab-column connections tested including same concrete compressive strength and ratio of the reinforcement. All slabs will be tested as a simply supported and subjected to punching loading by interior column. Test results show that the internal strengthening technique by using high tensile strength CFRP bars improves the bearing capacity of RC two-way slabs.

Based on the experimental results, it is possible to increase punching shear capacity by using internally reinforced with CFRP bars concentrated in slab-column zone, this increase is about (33-100%) compared with the unstrengthened (control) slab.

The effectiveness of the CFRP bars is depended substantially on distributed or arrangement manner in slab-column region.

Also, it is found that, the use of NSM CFRP bars is an effective technique to enhance shear capacity of SCC slab-column models and nearly provided the same efficiency of internal reinforcement.

Even efficient to increase the punching shear load, the top reinforcement of CFRP bars will not change the brittle-type punching shear failure mode compared with bottom CFRP bars reinforcement.

1- INTRODUCTION

Slabs-columns or flat plates, are solid concrete slabs of uniform depths that transfer loads directly to the supporting columns without the aid of beams or capitals or drop panels (**McCormac and Brown, 2014**)[1.] Flat plates are probably the most commonly used slab system today for multistory reinforced concrete hotels, motels, apartment houses, hospitals, and dormitories (**Varghese, 2009**)[2].

The greatest disadvantage of flat plate systems is the risk of brittle punching failure at the slab-column connection due to transfer of shear and unbalanced moments (**Zaghlal, 2009**).[3]

Although, the punching shear capacity of reinforced concrete flat plates can be increased by various means, their applicability is often limited, e.g., traditional shear reinforcing by means of stirrups is

applicable only to slabs with the depth greater than 150 mm according to (**ACI Committee 318-11**)[4]. Reinforcement using headed studs but this one need much time for construction, etc. (**Feretzakis**) [5].

Recently a new technique using of straight fiber reinforced polymer (FRP) bars to improve punching shear resistance and performance of the slab-column connections by internal strengthening; because a high strength to specific weight ratios of FRP bars reduce the complicated and heavily reinforced in slab-column connection in comparison with conventional reinforcement to perform the same strength, constructed quickly because of their simple formwork and reinforcing bar arrangements to save in construction time and they give the most flexibility in the arrangement of columns and partitions; therefore, thinner concrete slabs can be obtained.

In recent years, the design of modern reinforced concrete structures has become more advanced, the designed shapes of structures are becoming increasingly complicated and heavily reinforced, at the time, and there is a shortage of skilled labor especially at construction sites. Furthermore, there is a need to save in construction time and dead load for foundations and also to eliminate problems associated with vibration. Therefore, the newly born Self Compacting Concrete (SCC) as an innovative building material will offer new possibilities and prospects (**Al-Shammary**) [6]. Also, it has been used under trade names, such as the Non-Vibrated Concrete (NVC), Super Quality Concrete (SQC) (**Al-Mishhadaniand Al-Rubaie, 2009**)[7].

It is a new type of high performance concrete with the ability of flowing under its own weight and without the need of vibrations (**Druta, 2003**) [8].

Okamura and Ozawa employed the following methods to achieve self-compactability : (1) Limited aggregate content; (2) Low water/powder ratio and (3) The use of superplasticizer (**Okamura and Ouchi, 2003**)[9].

2- OBJECTIVE OF RESEARCH

This paper presents an experimental study on the effect of internal strengthening by straight carbon fiber reinforced polymer (CFRP) bars on the punching shear resistance and overall behavior of slab-column systems and a new strengthening technique named near surface mounted (NSM) in two directions of slab under static loads. The basic objective of the present work is to study the fresh and some mechanical properties of SCC which will use in casting slab-column connection monolithically . Also, to study the effect of the length, location, arrangement or distribution of straight carbon fiber reinforced polymer (CFRP) bars and focusing this reinforcement in critical region; by using the same ratio of CFRP bars.

3- EXPERIMENTAL PROGRAM

3-1 Description of Specimens

Seven flat plate slabs, are constructed for this study using self compacting concrete (SCC) for a square slab (1100×1100 mm) in size, with a total thickness of (60mm) and (120×120mm) square column with (150mm) height, cast monolithically at the centre of the slab. The slab portion of these models is reinforced with bottom reinforced of deformed steel bar of (6mm) diameter distributed across the section (100mm C/C) in two directions. All slabs of geometrically and steel reinforcement are similar. The slabs are simply supported along all edges and the distance from C/C of support is (950mm) and loaded through a central column. **Figure (1)** illustrates all details of geometry and reinforcement scheme of the tested models

One control model (CS) without carbon fiber reinforced polymer (CFRP) bars as in **Figure (1)** for comparison with others modes. While others models containing same amount of CFRP bars of 6mm diameter are listed below in **Table (1)** and shown in **Figure (2)**.

The specimen (SRUF1-NSM) is strengthening by using NSM technique which described according to the recommendation of **(ACI 440.2R-08)**[10]: ply wood strips with a size of 10mm width and 20mm depth were installed at the bottom of the wooden mould to provide two similar grooves in two directions before casting. The slabs were cured in air-conditioned laboratory for 28 days and then the ply wood strips were removed; the grooves were removed of any dirt by blowing. the grooves are then filled halfway with epoxy paste then CFRP bars is placed in the groove lightly pressed so induced the epoxy penetration around the bars then filled with more epoxy and the surface is leveled. The epoxy paste is allowed to cure for at least 7 days before the slabs are tested; **Figure (3)** show the mould and the SRUF1-NSM model.

3-2 Material Properties
3-2-1 Cement
Ordinary Portland cement (OPC) (type I) was used in this study. The cement was produced by United Cement Company (UCC) commercially known as "Tasluja-Bazian". The **Table (2)** shows physical properties and chemical analysis of this cement, which comply with the Iraqi Standards **(IQS) No.5:1984** [11] requirements.

3-2-2 Fine Aggregate
Natural sand brought from Al-Ukhaider region was used in this study. The results conformed to the **IQS No.5:1984 Zone 2**[12] showed that the physical and chemical properties and the grading are listed in **Table (3)** and **Table (4)**; respectively.

3-2-3 Coarse Aggregate
Rounded coarse aggregate of maximum aggregate size of 9.5 mm from Al-Nebai quarry are used. **Table (5)** show the grading of this aggregate, which conforms to the Iraqi Specification **No.45/1984**[12]. The physical and chemical properties are illustrated in **Table (6)**.

3-2-4 Mineral Admixture (Silica Fume)
Silica fume used in this study was Egypt production under trade name (Sika Fume®-HR). The physical and chemical properties of silica fume used are shown in **Table (7)**, it was conformed to the requirements of **(ASTM C1240-05)**[13].

3-2-5 Superplasticizer
The superplasticizer used in this study was a Glenium 51 (High Range Water-Reducing Concrete Admixture). It is conformed to **(ASTM C494-05)** [14]; in order to achieve flowability with silica fume to produce SCC. **Table (8)** shows the typical properties of Glenium 51according to manufacturer.

3-2-6 Water
Tap water was used for both mixing and curing of concrete in this work.

3-2-7 Steel Reinforcement
Deformed steel bars (6) mm in diameter are used in this study. It was obtained from BRC Turkish production. Three specimens of each bar are tested under tension according to **(ASTM A615/A615M-05a)**[15] requirements. The results of testing steel reinforcement are summarized in **Table (9)**.

3-2-8 Carbon Fiber Reinforced Polymer (CFRP) Bars

Aslan 201 CFRP bar of 6 mm nominal diameter is used for NSM technique. The certificate of analysis for the physical properties was provided by the manufacturer, **(Hughes Brothers)**[16], as shown in **Table (10)**.

3-2-9 Epoxy Adhesive

The Epoxy Adhesive of Sikadur–30 is the most suitable adhesive material used with CFRP bar in NSM technique. The adhesive type consists of two compounds, compound A and compound B. The mix ratio was 3:1 as A:B. Its main properties as supplied by the manufacturer are shown in **Table (11)**.

3-3 Mix Proportions

The SCC mix proportions are designed according to The European Guidelines for Self Compacting Concrete 2005 **(EFNARC, 2005)** [17].Mix design of SCC must satisfy the criteria on filling ability, passability and segregation resistance in addition to compressive strength which is equal 30 MPa. Therefore, trial mixes are prepared by accurate weighing and the proportions of materials are modified to obtain a satisfactory self-compactability by evaluating fresh concrete tests. The details of the selected mix is given in **Table (12)**.

3-4 Mixing Procedures and Tests of Fresh Concrete

In this study Emborg's mixing procedure **(Emborg, 2000)** [18] is adopted in order to achieve the required workability and homogeneity of SCC mixes.

Several test methods are implemented in this study in order to ensure that SCC mixes meet these requirements. The requisite test methods reported by **(Schutter, 2005)** [19] and **(Kumar, 2006)** [20] are Slump Flow and $T_{50 \text{ cm}}$ Tests; L-Box Test and V-Funnel Test as shown in **Figure (4)**, the fresh properties result of the mix are shown in **Table (13)**. This table indicates that the results are within the limits.

3-5 Testing of Hardened Concrete

3-5-1 Compressive Strength Test: The compressive strength of concrete ($f_{c'}$) was tested on 300×150 mm concrete cylinders according to **(ASTM C39/C39M-05)** [21] while, The compressive strength of concrete (f_u) was tested on (150) mm concrete cylinders according to **(BS 1881-part 116:2000)** [22]

3-5-2 Splitting Tensile Strength Test: The splitting tensile strength (f_{sp}) is determined according to the procedure outlined in **(ASTM C496/C 496M-04)** [23].

3-5-3 Flexural Strength Test: Concrete prisms of dimensions ($100 \times 100 \times 400$) mm are cast according to **(ASTM C 78-02)** [24] procedure and tested to finding flexural tensile strength (f_r).

3-6 Casting and Curing of the Slab-Column Models

According to **(ASTM C 192/C 192M-05)** [25], all moulds were poured with SCC and cured as shown in **Figure (5)**

3-7 Testing Setup and Instrumentation

The punching test of slab-column models are performed by subjecting to a central punch load over the central column 120×120 mm by applying to the top face of slabs by a hydraulic jack of the universal testing machine of 2000 kN under monotonic loads up to ultimate load, see **Figure (6)**.

The corners of slabs are supported by means of eight steel members, two for each corner as a steel levers to prevent lifting of the corners during the loading to satisfy closely the boundary conditions. The slabs were instrumented with three vertical dial gauges of 50 mm and accuracy of (0.01) mm at mid-span, at mid one quarter and at mid one side to monitor the deflection as shown in **Figure (7)**. The strain of concrete are measured by an ELE extensometer with accuracy of 0.002 mm. Many pairs of demec discs are used to monitor the strain concrete at selected levels of loading at several points on the tension face of slab; arrangement and distribution of these demec discs are shown in **Figure (7)**. The load was applied to the slab at a rate of 250 N/sec by means of the hydraulic jacks. At each load interval (5 kN), the cracks width was measured by crack meter (Elecometer 900) with an accuracy of 0.02 mm; and crack propagation were marked. All instruments used in testing are shown in **Figure (8)**

4- Experimental Results and Discussion

4-1 Mechanical Properties of Each Slab-Column Models

The mechanical properties for each slab-column model are listed in **Table (14)** from experimental work except the modulus of elasticity which is calculated according **(ACI318-11)** [26] from **Equation (1)**.

$$E_c = 4700\sqrt{f_{c'}} \tag{1}$$

It appears in **Table (14)** that, the proportion between cube and cylinder compressive strength ($f_{cu}/f_{c'}$) for SCC is about 1.215. From experimental result of hardened test of SCC, The compressive cylinder and cube strength are ranged between (31.4-32-2) and (37.9-39.1), respectively. Also, the splitting tensile strength and flexural strength are ranged between (2.37-2.44) and (3.49-3.54), respectively.

4-2 Cracking Behavior

The first crack appears around the sides of the column on the tension face of the slab without CFRP bars about (28%) in control slab (CS) of the ultimate failure load . On the other hand, the first crack of all tested slabs strengthening internally with CFRP bars appears in the tension face of the slab about (24.1-26.7%) of the ultimate failure load. While, the first crack of model which strengthened by CFRP bars NSM technique appears at 20.7% of the ultimate failure load in the tension face of the slab around the sides of the column a crossing through the NSM bars. **Table (15)**, listed the first loads at tension and compression face of slab-column models, an increase in comparison with CS model and the percentage of the ultimate failure load.

As the load is increased after the formation of the first crack, more cracks begin to appear and move towards the edge of the slab. In the compression face of the tested slabs, there are cracks that appear away from the edge of the column. Except the slab (CS), cracks are found round the edge of the column only. The test results show that using CFRP bars in control slab (CS) increases the first cracking load in tension face between (14.3-90.5%) over the control slab without CFRP bars due to the increase in flexural capacity. The mechanism of development of cracks is almost the same for all models. The cracking pattern at failure for tension and compression face of each model is shown in **Figure (9)**. In slab-column models the use of CFRP bars reinforced, increased the size of the shear failure surface compared with control model CS.

The maximum crack width was monitored throughout the test to recording the width of crack with increasing load (at each 5 kN) starting from first crack until near failure of the slab-column models. The width of first crack of slab-column models in tension face ranged between (0.03-0.08) mm.

While, the width of crack in compression face increase quickly after appearing and ranged between (0.07-0.11) mm as shown in **Table (15)**.

In general, slabs with CFRP bars have maximum crack width smaller than the control slab (CS) during the same stage of loading as shown in **Figure (10)**.

At failure, the maximum crack width are (2.8, 2.26, 2.6, 2.21, 2.5, 2.48 and 2.16) mm for (CS, SRUF1-NSM, SRUT, SRUF1, SROF, SRDF and SRUF2), respectively.

The results show that, the maximum crack width decreases about (29.6%) in SRUF2 model in comparison with CS model due to concentrated CFRP bars reinforcement in the immediate column region with flexural steel reinforcement, its restraining effect will increase and that reflects the decrease in the crack width.

4-3 Load-Deflection Curves

The recorded ultimate loads, deflections and failure mode for all slab-column models are presented in **Table (16)**.

As the load on a test model was increased, the load-deflection behavior was noticed to have three distinguished stages: *the elastic stage* is an initial straight portion of the load-deflection curve, *elastic-plastic stage* is a nonlinear portion with distinct change in slope with increasing deflections and *plastic stage* is also a nonlinear portion but has characteristics in which a slight increase in load results in a larger deflection.

The structural behavior of tested slab-column models are referred to here by their experimental load versus deflection as shown in **Figure (11)**

The initial change of slope of the load-deflection curves for all series started between (10.5-20) kN. This change in slope indicated the first cracking load. Beyond that, all models behave in a rather certain manner.

Generally, the use of CFRP bars reinforcement internally to improve punching shear capacity of slab-column region is successfully due to enhanced strength above the punching shear capacity and increased stiffness as shown in **Figure (11)** and as a result in **Table (16)** that showed the increased ranged between (25.3-100%) for different distribution of same amount of CFRP bars.

For the slab-column model CS, which is slab without CFRP bars, the experimental ultimate load capacity for this slab is 37.5 kN. An increasing in the ultimate load of SRUF2 is 100%. whereas, the ultimate load of SRUF1 and SRUF1-NSM is higher than that of the reinforced concrete slab-column model CS by 81.3% and 80%, respectively. It is evident from this result and according to **Figure (11)** that distribution of flexural CFRP bars reinforcement the slab-column models (SRUF2, SRUF1 and SRUF1-NSM) had higher punching shear capacities, higher loads at first cracking in tension and compression face as mentioned previously, and higher postcracking stiffnesses. Also, it was noted that the SRUF1-NSM model which is strengthening by using NSM technique in two directions gave approximately the same efficiency to internal CFRP bars used in SRUF1model.

In slab-column model SROF, the contribution of the compressive reinforcement of CFRP bars to the punching shear capacity was 33.3% which is small comparison with other distribution manner of CFRP bars but reduce the central deflection at failure.

SRDF model gave improving in punching shear capacity more than SROF by only 8% due to the small region that distributed the CFRP bars through it.

Replacing the CFRP bars with steel bars in SRUT model reduced the punching strength with about 44.7% because CFRP bars have high tensile strength is 2704 MPa compared with steel reinforcement. Also, SRUT model gave lower central deflection at failure by 15.7% due to lower modulus of the CFRP bars 163000 MPa compared with 200000 MPa for steel reinforcement.

The deflected shape for slab-column models at failure is different along sides lateral from diagonal of slabs as shown in **Figure (12)**.

4-4 Concrete Strain

The strains in the concrete at tension face of the tested slab-column models were measured by using a demic gauge along half one principal and diagonal axes of symmetry. **Figure (7)** shows the positions of demic points. From the **Figure (13)**, it can be seen that the concrete strain is small at the elastic stage as loading is applied, then it increases after the first crack when loading is continued.

In the distribution of strains, the increase of strains started from the center of the slab toward the punching shear cracks, in principal and diagonal axes of tension surface of slab. At failure, the maximum concrete strain is observed around the sides of the column on the tension face of the slab especially toward the diagonal of slabs which is the strains was more than that in the principal directions as shown in **Figure (14)**, **Figure (15)** and **Figure (16)**.

The presence of CFRP bars at the bottom tension zone surface of slab-column region increasing the tension strength and some tensile stresses were carried by CFRP bars, and this was reflected to reduce the strains in the bottom tension surface.

5-Conclusion

Based on the observed behavior and test results, the following conclusions are reached regarding the reinforced concrete slab-column models which improved punching shear resistance by using CFRP bars:

1- The majority beneficial of using SCC in casting slab-column model to ensure that adequate strength and durability are achieved due to capable of flowing through narrow column and extremely congested reinforcement, and provides a void-free surface. Insufficient compaction will lead to the inclusion of voids, which not only leads to a reduction in compressive strength but strongly influence the natural physical and chemical protection of embedded steel reinforcement afford by concrete.

2- The internally strengthened reinforced concrete slab-column model with CFRP bars show a significant increase in ultimate loads and the capacity of the slabs, this increase is about (33-100%) compared with the unstrengthened (control) slab.

3- The effectiveness of the CFRP bars is depended substantially on distributed or arrangement manner in slab-column region.

4-The concentration of the flexural steel reinforcement in the column vicinity, also increased the punching shear capacity.

5- Even efficient to increase the punching shear load, the top reinforcement of CFRP bars will not change the brittle-type punching shear failure mode compared with bottom reinforcement. This means, the punching shear capacity of slab-column model was controlled by bottom flexural reinforcement rather than top reinforcement.

6- NSM technique by CFRP bars in two direction of slab is very effective and nearly provided the same efficiency of internal reinforcement.

7- the use of CFRP bars reinforcement in strengthening the slab-column region, results in a higher punching shear strength, a greater postcracking stiffness, a more uniform distribution of the strains in addition to reduce it, and smaller crack widths at full service loading compared with unstrengthening slab.

6- References

[1] McCormac, J.C. and Brown, R.H., 2014 " Design of Reinforced Concrete", 9th Edition, John Wiley & Sons, Inc. 742PP.

[2] Varghese, P.C., 2009 "Advanced Reinforced Concrete Design", 2nd Edition Indian Institute of Technology Madras, Anna University.

[3] Zaghlal, M.Y.A., 2009 "Structural Department Punch Resistance of Slab Column Connection Under Lateral Loads", M.Sc., Zagazig University.

[4] ACI Committee 318, 2011 "Building Code Requirements for Reinforced Concrete Design", American Concrete Institute, Detroit. MI. USA.

[5] Feretzakis, A., 2005 "Flat slabs and punching shear: Reinforcement Systems" M.Sc. thesis, Univsity of Dundee, Dundee, UK.

[6] Al-Shammary, D. Sh. A., "Some Properties of Porcelanite Lightweight Aggregate Self-Compacting Concrete," MSc, Thesis, University of Technology, Baghdad, Iraq, 2006, 94 pp.

[7] Al-Mishhadani, S.A. and Al-Rubaie, M.F., "A Data Base for Self-Compacting Concrete in Iraq", Department of Building

[6] Al-Mishhadani, S.A. and Al-Rubaie, M.F., *"A Data Base for Self-Compacting Concrete in Iraq"*, Department of Building and Construction Engineering, University of Technology, Iraq, Eng. & Tech. Journal Vol.27 No.6, 2009. www.pdffactory.com.

[8] Druta, C., "Tensile Strength and Bonding Characteristics of Self-Compacting Concrete", MSc. Thesis, Louisiana State University and Agricultural and Mechanical College, August, 2003.

[9] Okamura, H. and Ouchi, M., "Self-Compacting Concrete", Journal of Advanced Concrete Technology, Japan, Vol.1, No.1, pp.5-15, April, 2003.

[10] ACI Committee 440, 2008 "Guide for the Design and Construction of Externally Bonded FRP Systems for Strengthening Concrete Structures (ACI 440.2R-08)", ACI Manual of Concrete Practice, American Concrete Institute, Farming Hills, U.S.A.

[11] Iraqi Specification, No.5, "Portland Cement", Baghdad, 1984.

[12] Iraqi Specification, No.45, 1984 "Aggregate from Natural Sources for Concrete and Construction", Baghdad.

[13] ASTM standard, ASTM C 1240-05, 2005 "Standard Specification for Silica Fume Used in Cementitious Mixtures", pp. 1-7

[14] ASTM C 494/C 494M-05, 2005 "Standard Specification for Chemical Admixtures for Concrete", Annual Book of ASTM Standards, American Society for Testing and Materials, Vol.04.02.

[15] ASTM A 615/A615M-05a, 2005 "Standard Specification for Deformed and Plain Billet-Steel Bars for Concrete Reinforcement", ASTM Committee A01 on Steel, Stainless Steel, and Related Alloys, West Conshohocken, PA 19428-2959, United States, 5 pp.

[16] Hughes Brothers, 2012 "Carbon Fiber Reinforced Polymer (CFRP) Rebar Aslan 200", Manufacturer Report.

[17] EFNARC: The European Federation of Specialist Construction and Concrete System "The European Guidelines for Self-Compacting Concrete; Specification, Production and Use", pp.1- 63, May, 2005. www.efnarc.org.

[18] Emborg, M., "Self-Compacting Concrete: Mixing and Transport", Brite EuRam, Final Report of Task 8.1, pp.1-65, June, 2000.

[19] Schutter, G.D., "Guidelines for Testing Fresh Self-Compacting Concrete", European Research Project Published by: Systematic Pan-European inter-Laboratory, pp.1-23, September, 2005.

Available on websites: www.efca.info or www.efnarc.org

[20] Kumar, P., "Self-Compacting Concrete: Methods of Testing and Design", IE (I) Journal-CV, Vol.86, pp.145-150, February, 2006.

[21] ASTM C 39/C 39M-05, 2005 "Standard Test Method for Compressive Strength of Cylindrical Concrete Specimens," Annual Book of ASTM Standards, Vol. 04.02 Concrete and Aggregates, West Conshohocken, PA, United States, 7 pp.

[22] BS 1881-Part 116:1983, 2000 "Method for Determination of Compressive Strength of Concrete Cubes," British Standards Institute BSI, London, 11pp.

[23] ASTM C 496/C 496M-04, 2004 "Standard Test Method for Splitting Tensile Strength of Cylindrical Concrete Specimens," Annual Book of ASTM Standards, Vol. 04.02 Concrete and Aggregates, West Conshohocken, PA, United States, 5 pp.

[24] ASTM C 78-02, "Standard Test Method for Flexural Strength of Concrete (Using Simple Beam with Third-Point Loading)", Annual Book of ASTM Standards, American Society for Testing and Materials, 2002.

[25] ASTM C 192/C 192M-05, 2005 "Standard Practice for Making and Curing Concrete Test Specimens in the Laboratory", Annual Book of ASTM Standards, American Society for Testing and Materials, pp.1-8.

[26] ACI Committee 318, 2011 "Building Code Requirements for Reinforced Concrete Design", American Concrete Institute, Detroit. MI. USA.

Table (1): Models identification

Symbols	Refer to
CS	Control slab without CFRP bars as in Figure1
SRUF1	Slab reinforced with CFRP bars with the same level of slab steel reinforcement, arrangement 1
SRUT	Slab reinforced with steel bars with the same level of slab steel reinforcement
SRUF1-NSM	Slab reinforced with CFRP bars by NSM technique
SROF	Slab reinforced with CFRP bars over the level of slab steel reinforcement
SRDF	Slab reinforced with doubly layer of CFRP bars, one layer over the level of slab steel reinforcement and the other with the same level.
SRUF2	Slab reinforced with CFRP bars with the same level of slab steel reinforcement, arrangement 2

Table (2): Chemical analysis and physical properties of the cement

Chemical Analysis			
Compound Composition	**Chemical Composition**	**Percentage by Weight**	**Limits of IOS No.5:1984**[7]
Lime Oxide	CaO	61.23	-
Silica Dioxide	SiO_2	20.898	-
Alumina Oxide	Al_2O_3	5.66	-
Iron Oxide	Fe_2O_3	3.38	-
Magnesia Oxide	MgO	2.76	$\leq$ 5.0%
Sulfate Trioxide	SO_3	2.34	$\leq$ 2.5% if C3A <5% $\leq$ 2.8% if C3A >5%
Loss on Ignition	L.O.I	1.29	$\leq$ 4.0%
Insoluble Residue	I.R	0.70	$\leq$ 1.5%
Lime Saturation Factor	L.S.F	0.77	0.66-1.02
Main Compounds (Bogue's Equation) Percentage by Weight of Cement			
Tricalcium Silicate (C_3S)		40.31	
Dicalcium Silicate (C_2S)		31.11	
Tricalcium Aluminate (C_3A)		9.49	
Tetracalcium Alumino ferrite (C_4AF)		10.43	
Physical Properties			
Physical Properties		**Test Results**	**Limits of IOS No.5:1984**[7]
Specific Gravity		3.15	-
Fineness: Specific Surface, Blaine . (cm^2/g)		3160	$\geq$ 2300
Setting Time (Initial) (min.)		128	$\geq$ 45
Setting Time(Final) (min.)		245	$\leq$ 600

Table (3): Physical and chemical properties of fine aggregate

Properties	Test Results	Limits of IOS No.45:1984[8]
Specific Gravity	2.62	-
Sulfate Content SO3	0.37%	$\leq$ 0.5%
Absorption	0.88%	-
Material finer than 75 μm (Sieve No. 200) (%weight)	3.54%	$\leq$ 5%
Fineness Modulus	2.581	-

Table (4): Grading of fine aggregate

Sieve Size (mm)	Passing %	Limits of IOS No. 45:1984 for Zone 2[8]
10	100	**100**
4.75	93.8	**90-100**
2.36	83.1	**75-100**
1.18	75.1	**55-90**
0.60	58	**35-59**
0.30	29	**8-30**
0.15	2.9	**0-10**

Table (5): Grading of coarse aggregate

Sieve Size(mm)	Passing %	Limits of IOS No. 45/1984[8]
14	100	**100**
10	100	**85-100**
5	18	**0-25**
2.36	0	**0-5**

Table (6): Physical and chemical properties of coarse aggregate

Properties	Test Results	Limits of IOS No.45/1984
Specific Gravity	2.6	-
Sulfate Content SO$_3$	0.08%	0.1% $\leq$
Absorption	0.68%	-
Clay Content	0.06%	2% $\leq$

Table (7): Physical and chemical properties of silica fume

Physical state	Fine powder.
Color	Grey
Odor	Characteristic.
pH value at 20°C	Non
Melting Point ^{o}C	160°C
Ignition point ^{o}C	365°C.
Density at 20°C	0.65 $\pm$ 0.1 kg/lit.
Thermal Conductivity	Low
Bulk Density	300 kg/m^3

Table (8): Typical properties of Glenium 51 from the manufacture company catalogue

Main Action	Concrete Superplasticizer
Color	Light brown
pH. Value	6.6
Form	Viscous liquid
Subsidiary Effect	Hardening
Relative Density	1.1 at 20°C
Viscosity	128 $\pm$ 30 cps at 20°C
Transport	Not classified as dangerous
Labeling	No hazard table required

Table (9): Test results properties of steel bars

Φ (mm)	Area As (mm^2)	Perimeter (mm)	Weight (Kg/m)	Pattern	Yield strength fy (MPa)	Ultimate strength fu (MPa)	Yield strain	Ultimate strain
6	28.3	18.86	0.230	C*	556	767	0.0027	0.049

(C* deformation pattern C consists of diagonal ribs inclined at an angle 60 degree with respect to the axis of the bar),

Table (10): Aslan 201 CFRP rebar physical properties

Item	Standards	Result	Test method
Barcol Hardness	≥50	54.0	ASTM D2583
Tensile Strength, MPa (Average-3.0 Sigma per ASTM D7205)	≥2068	2704	ASTM D7205
Modulus of Elasticity, GPa (Average Value)	≥124	163	ASTM D7205
Ultimate Strain	0.017	0.017	ASTM D7205

Table (11): Technical properties of bonding materials

Properties	Sikadur - 30
Tensile strength (MPa)	26 - 31 Mpa
Full cure, days	7(at +35°C)
Compressive E-modulus GPa	9.6 Gpa (According to ASTM D695)
Shear Strength	18 MPa

Table (12): Mix proportion

Cement kg/m^3	Sand kg/m^3	Gravel kg/m^3	Sika Fume% Wt. of Cement	Water kg/m^3	SP% Wt. of Cement	w/c Ratio	w/p Ratio	$f_{c'}$ (28day) MPa
385	800	800	5%	194	0.8%	0.530	0.504	31.98

Table (13): Results of workability tests of the SCC

Method		Result	Property	Limitations [13]
Slump Flow	**(D) mm**	780	Filling ability	**650 – 800**
	(T$_{50\ cm}$) sec.	3.4		**2 – 5**
V-Funnel	**(T$_v$) sec.**	9.1	Filling ability	**6 – 12**
	Time increase, (T$_{v\ 5\ min.}$) sec.	2.2	Segregation resistance	**+ 0-3**
L-Box (BR)	**-**	0.88	Passing ability	**0.8 – 1.0**

Table (14): Mechanical properties of slab-column models

Model Symbol	$f_{c'}$ MPa	f_{cu} MPa	f_{sp} MPa	f_r MPa	E_c GPa
CS	32.0	39	2.42	3.53	26.6
SRUF1	31.5	38.4	2.37	3.52	26.4
SRUT	31.4	37.9	2.41	3.49	26.3
SRUF1-NSM	31.9	38.6	2.44	3.50	26.5
SROF	31.7	38.1	2.40	3.54	26.5
SRDF	31.5	38.4	2.38	3.51	26.4
SRUF2	32.2	39.1	2.42	3.50	26.7
Average	31.7	38.5	2.41	3.51	26.49

Table (15): Cracking and ultimate loads

Model Symbol	1st Crack in Tension Face		Increase in PR_T, %	1st Crack in Compression Face		Increase in PR_C, %	Ultimate Load P_U (kN)	PR_T/P_U%	PR_C/P_U%
	Load PR_T (kN)	Width mm		Load PR_C (kN)	Width mm				
CS	10.5	0.08	---------	23	0.11	---------	37.5	28.0	61.3
SRUF1	17	0.04	61.9	50	0.09	117.4	68.0	25.0	73.5
SRUT	12	0.06	14.3	38	0.07	65.2	47.0	25.5	80.9
SRUF1-NSM	14	0.05	33.3	50	0.09	117.4	67.5	20.7	74.1
SROF	12.5	0.06	19	45	0.07	95.7	50.0	25	90.0
SRDF	13	0.04	23.8	40	0.07	73.9	54.0	24.1	74.1
SRUF2	20	0.03	90.5	65	0.08	182.6	75.0	26.7	86.7

Table (16): Test result of slab-column models

Model Symbol	Ultimate Deflection (mm)			Ultimate Load (kN)	Increase in Ultimate Load Over CS,%	Failure Mode
	Central	Mid of Side	Quarter			
CS	17.23	12.35	9.85	37.5	---------	Punching shear
SRUF1	21.23	16.85	13.82	68	81.3	Punching shear
SRUT	18.35	11.88	10.14	47	25.3	Punching shear
SRUF1-NSM	22.1	15.01	10.35	67.5	80	Punching shear
SROF	18.8	16.19	11.6	50	33.3	Punching shear
SRDF	18.25	15.89	12.56	54	44	Punching shear
SRUF2	22.23	16.85	13.73	75	100	Punching shear
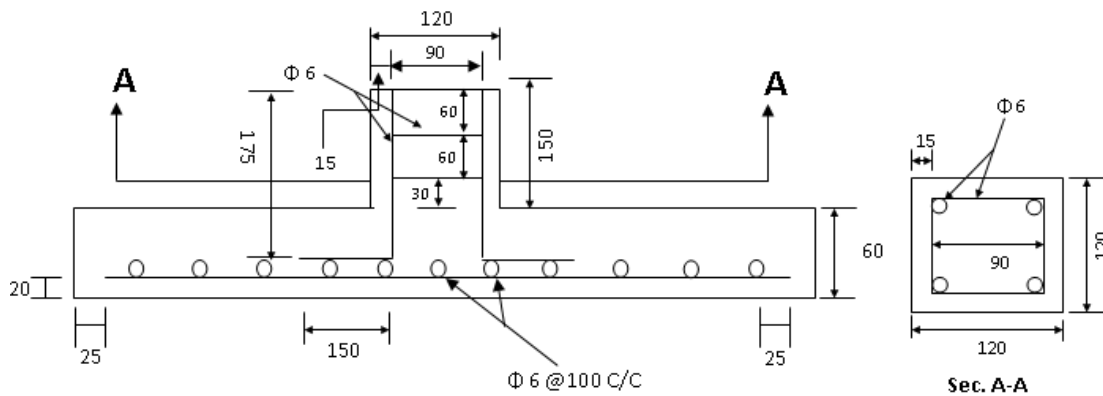
Figure (1): Details reinforcement of the slab-column model (all dimentions are in mm)
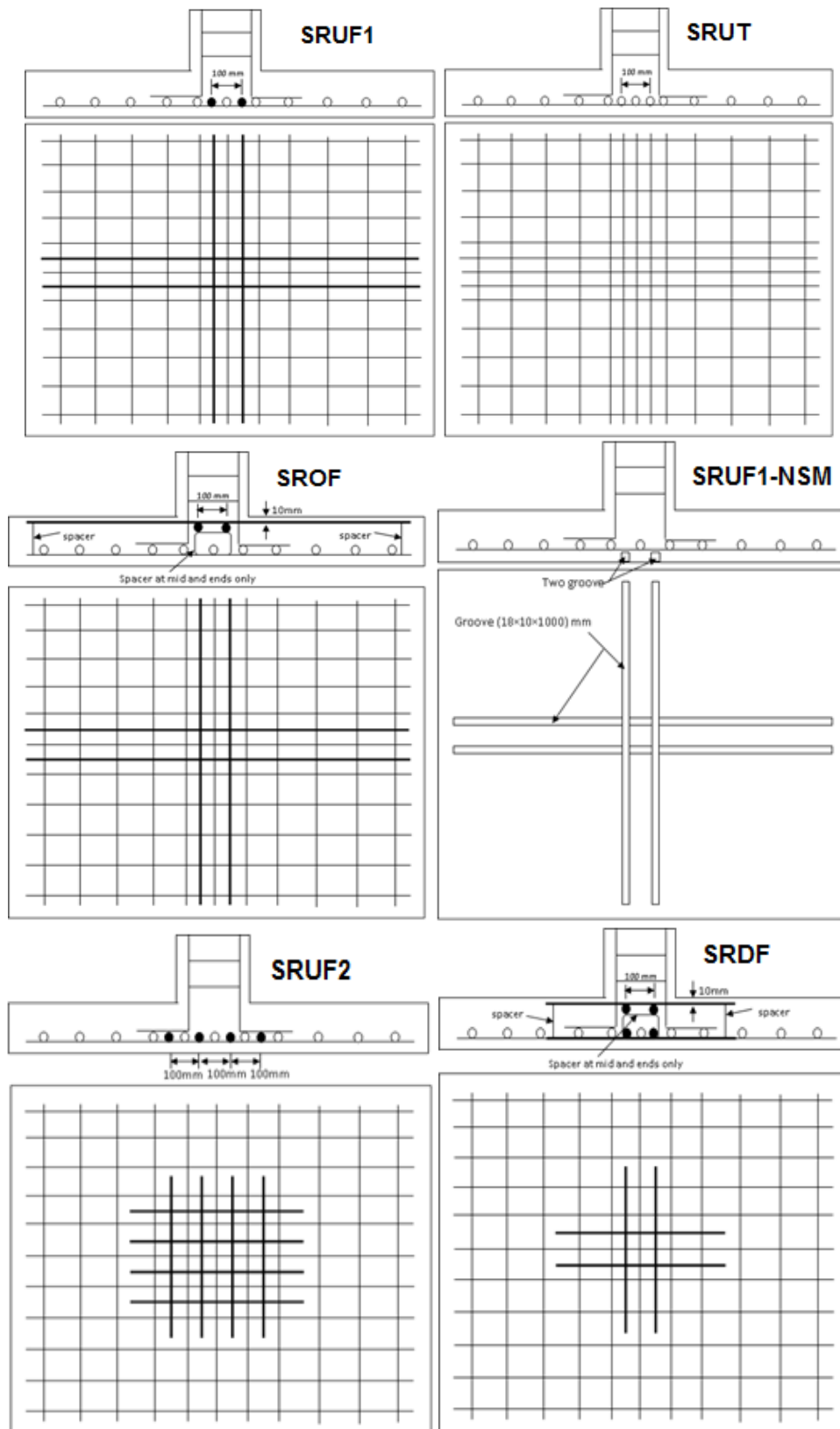
Figure (2): Details of the slab-column models

Figure (3): The mould and the SRUF1-NSM model

V-Funnel   L-Box   Slump Flow

Figure (4): Tests of fresh self compacting concrete

Tying of steel and moulds preparation

Casting process

Curing process and paint

Figure (5): Casting and curing conditions

Figure (6): Apparatus of the testing of slab-column models
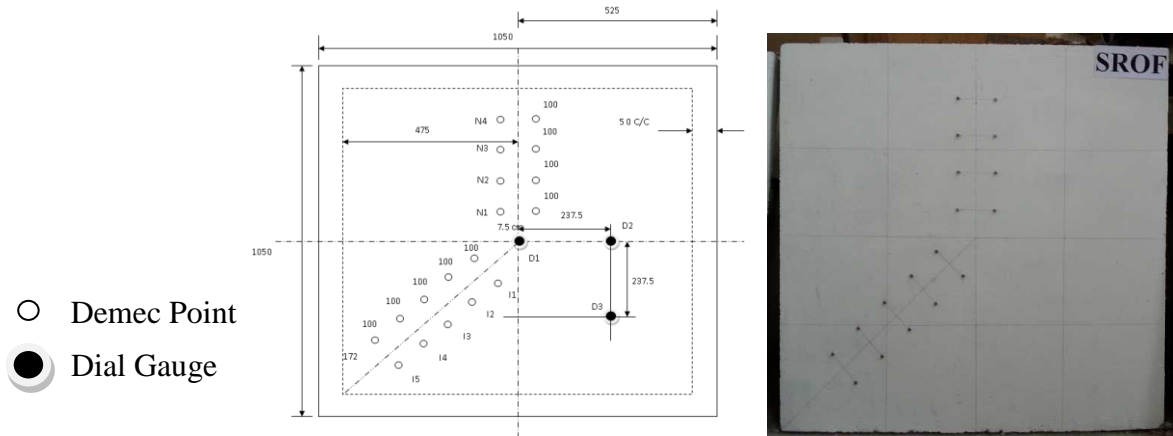
Figure (7): Configuration of demec points for strain and dial gauge for deflection

Dial gauge   ELE extensometer and demec discs   Elecometer 900

Figure (8): Instruments that used in testing
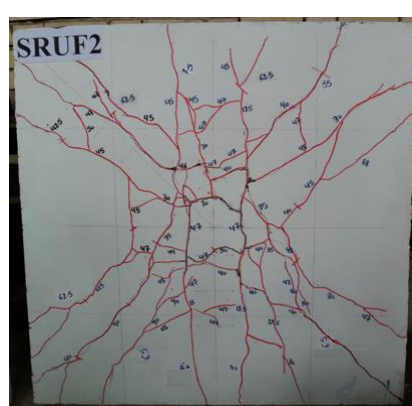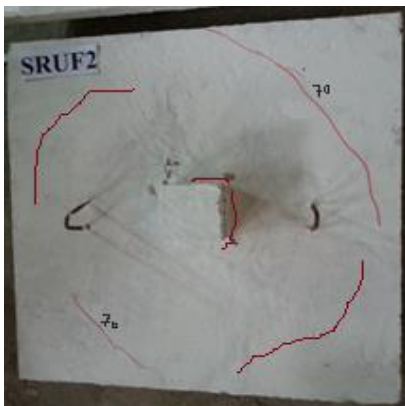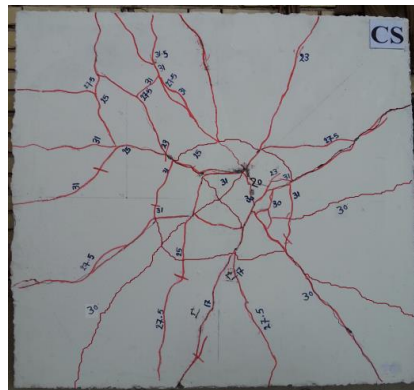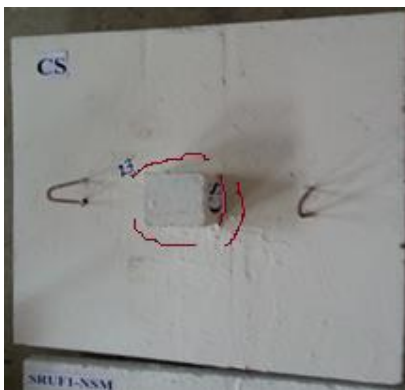
Figure (9): Cracks pattern at failure for all models
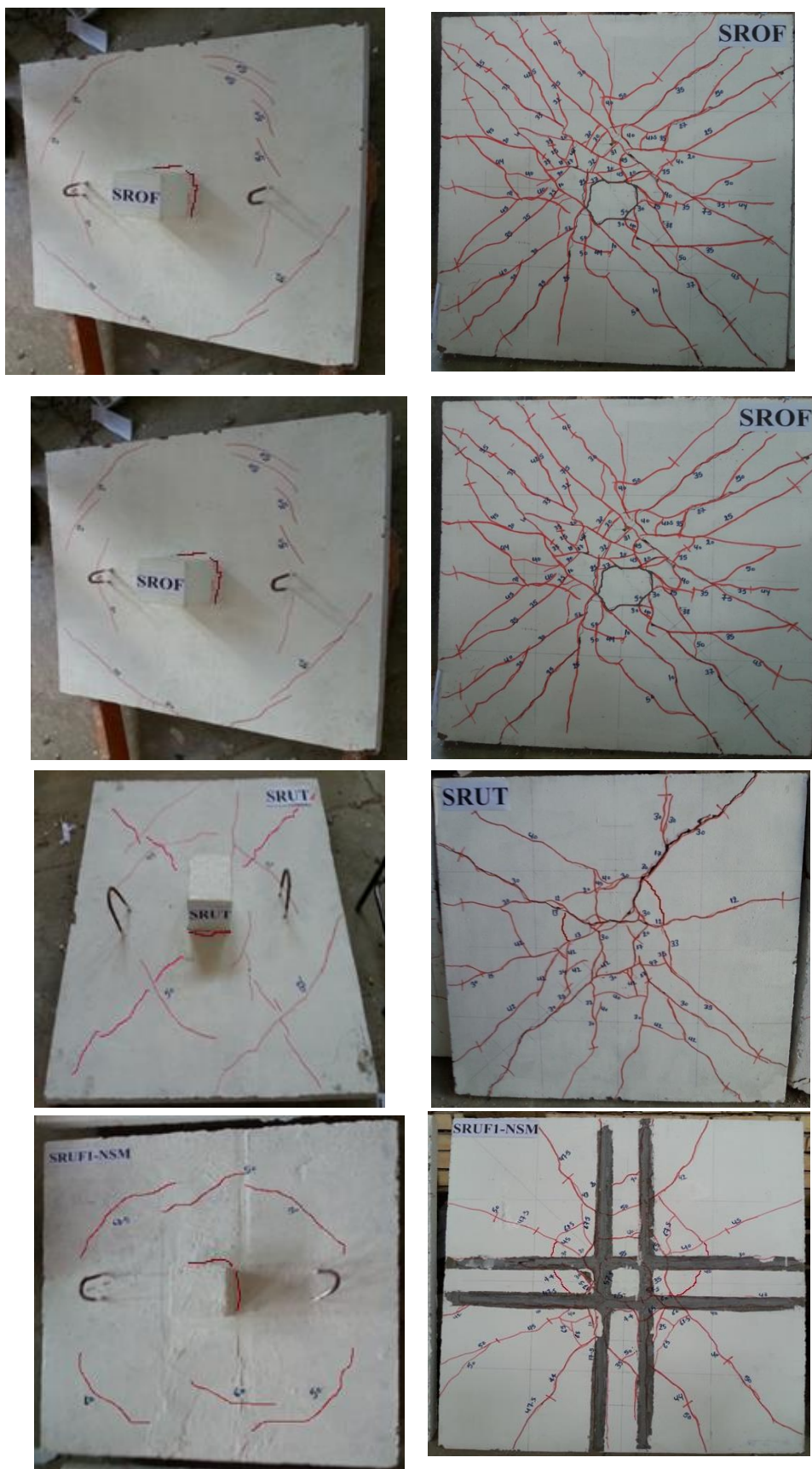
Figure (9): Continued
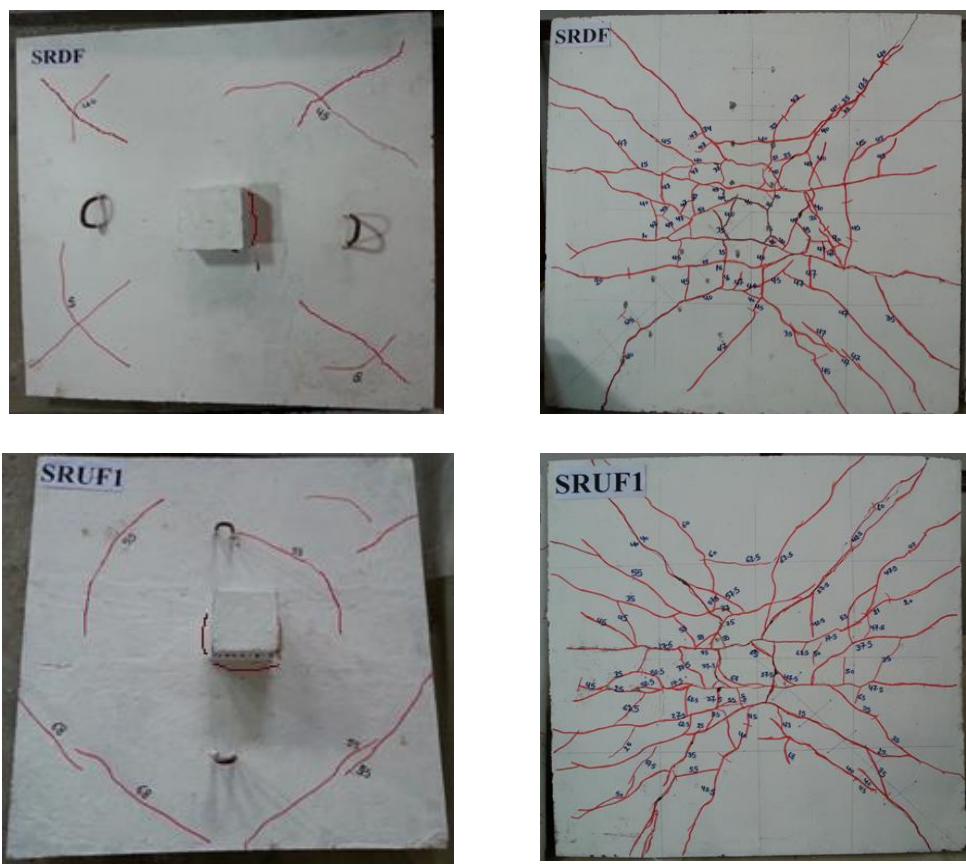
Figure (9): Continued
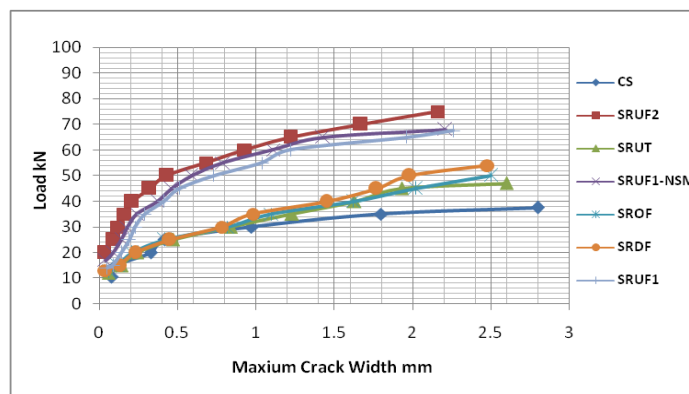
Figure (10): Maximum crack width-load curves for slab-column models
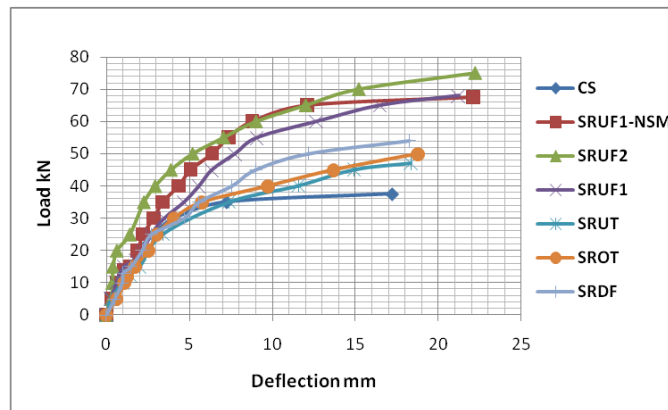
Figure (11): Load versus mid span deflection for all slab-column models
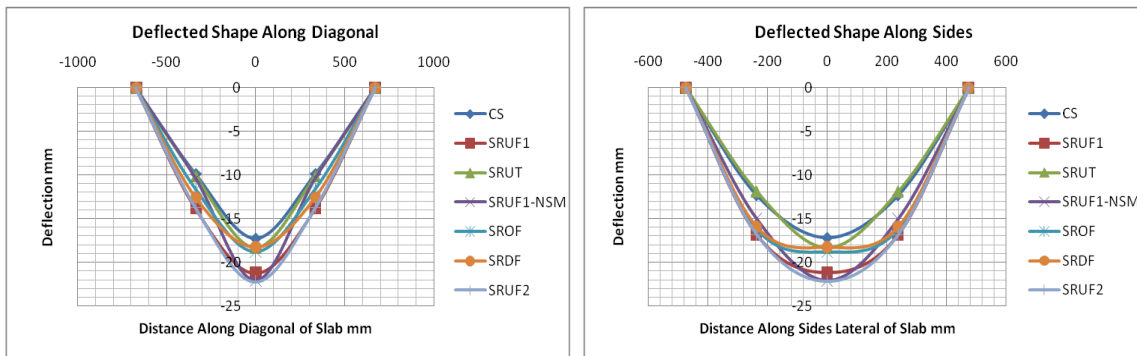
Figure (12): Deflected shape at failure for all slab-column models
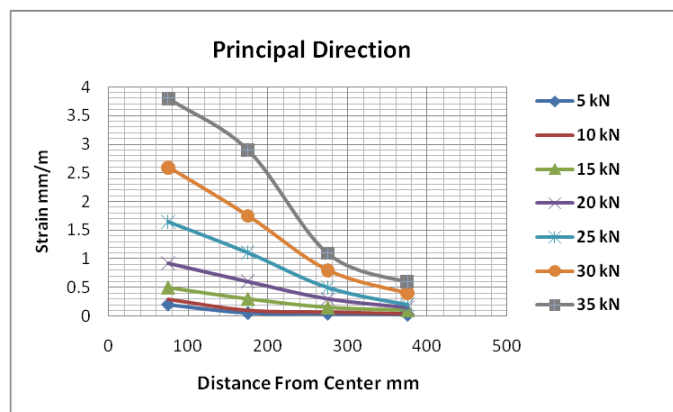
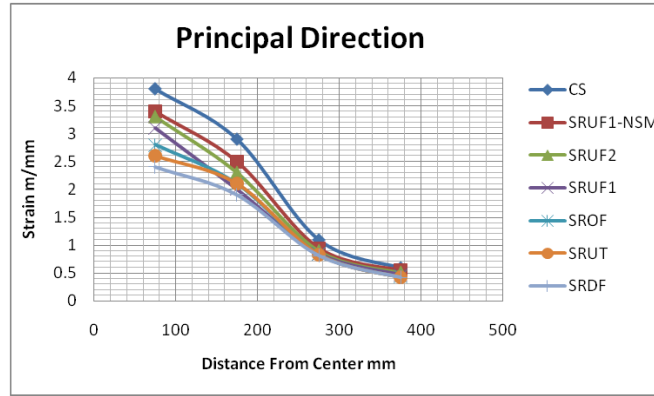**Figure (13):** Tensile strain versus distance along lateral sides of CS-Model

Figure (14): Tensile strain versus distance along lateral sides of all models
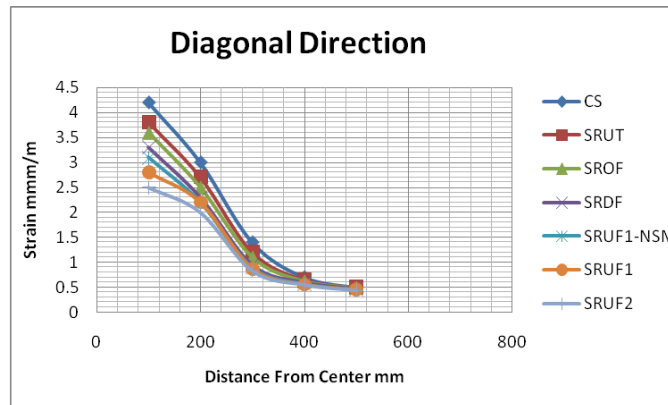

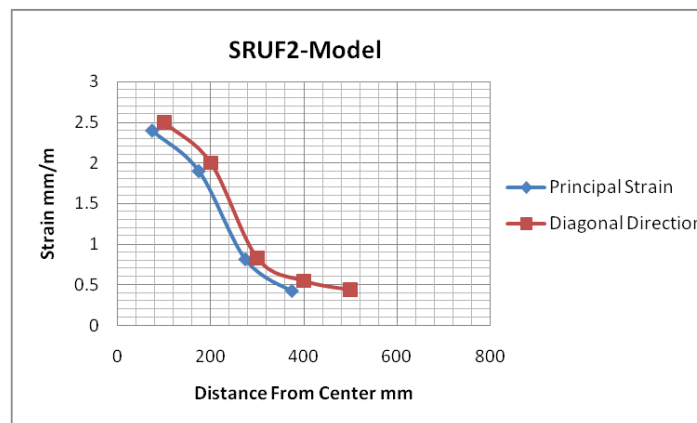**Figure (15):** Tensile strain versus distance along diagonal axis of all models

Figure (16): Tensile strain versus distance for SRUF2 model